Jung *et al. Applied Biological Chemistry* (2023) 66:6
https://doi.org/10.1186/s13765-022-00761-3

KSABC
The Korean Society for Applied Biological Chemistry

ARTICLE

Open Access

Effect of traditional herbal medicine, danggui-yukhwang-tang, on post-menopausal weight gain in ovariectomized high-fat diet rats

Dong Ho Jung†, Hyun Yang†, Joo Tae Hwang and Byoung-Seob Ko*

Abstract

The decrease in estrogen due to menopause leads to impaired lipid metabolism and is closely related to the increase in metabolic syndrome due to weight gain. Hormone replacement therapy is effective for menopause, but with an increased risk of side effects. Danggui-yukhwang-tang (DYT) is a traditional drug, comprising seven herbs, used to treat diseases like slight fever with sweating, blood-flow disorders, and neurasthenia. However, the effect on menopausal obesity has not been reported. This study aimed to investigate the inhibitory effect of DYT on weight gain in female rats fed a high-fat diet after ovariectomy. Adipocyte differentiation was effectively reduced by DYT in 3T3-L1 cells, and the mRNAs of *PPARγ*, *C/EBPα*, and *FABP4*, which are adipogenesis-related genes, were reduced. In the in vivo study, OVX and HFD elevated body weight; however, its induction significantly decreased in the DYT-treated groups. The serum lipid profile was also examined, and DYT treatment significantly decreased LDL-cholesterol, triglyceride, and total cholesterol levels compared with the OVX and OVX + HFD groups. DYT treatment effectively reduced the temperature(s) of the tail and body in the rats. The study demonstrates that DYT inhibits adipogenic differentiation, hypercholesterolemia, and weight gain in a post-menopausal rat model by regulating adipogenic markers (PPARγ, C/EBPα, FABP4) and the serum lipid profile in OVX + HFD rats.

Keywords Danggui-yukhwang-tang (當歸六黃湯, Dāngguīliùhuángtāng), Menopausal syndrome, Adipogenic differentiation, Obesity

Introduction

The decline in ovarian activity due to natural aging causes estradiol loss, clinically diagnosed as 'menopause,' when there is no menstruation for one year. It mainly occurs between the ages of 45 and 55, and the number of menopausal patients worldwide is expected to increase due to the extension of women's life expectancy [1–3]. Women diagnosed with menopause complain of various symptoms such as vasomotor symptoms (hot flashes and night sweats), osteopenia, osteoporosis, mental disorders, and sexual dysfunction [4]. Hormonal decline is closely associated with obesity, type 2 diabetes, and impaired lipid metabolism, which may contribute to weight gain and the pathogenesis of metabolic syndromes including cardiovascular disease (CVD) [5, 6].

Proliferator-activated receptor γ (PPARγ) and CCAAT/enhancer-binding protein α (C/EBPα) are key regulators of adipocyte differentiation and lipid accumulation. These adipogenic factors are directly implicated in adipogenesis pathways in adipocytes, including fatty acid-binding protein 4 (FABP4) and fatty acid synthase (FAS) [7]. Several studies have reported that the activity of the estrogen receptor α (ERα), a receptor for 17β-estradiol, decreases adipogenesis and lipid

†Dong Ho Jung and Hyun Yang contributed equally to this work

*Correspondence:
Byoung-Seob Ko
bsko@kiom.re.kr
KM Convergence Research Division, Korea Institute of Oriental Medicine (KIOM), 1672 Yuseong-daero, Yuseong-Gu, Daejeon 34054, Republic of Korea

accumulation through inhibition of PPARγ activity and decreases the activity of lipolytic enzymes due to ERα-induced upregulation of α-adrenergic receptors (αAR) [8, 9]. Therefore, 17β-estradiol (E_2) deficiency upregulates the expression of adipogenic genes required for energy storage while downregulating β-oxidation-related genes for energy production as the body's fuel source. This phenomenon causes negative fat and energy metabolism changes, resulting in an imbalance between them, eventually leading to obesity [10]. In addition, hot flashes are also a symptom with a high incidence in menopausal women. A study on the association between hot flashes and obesity showed that increased abdominal fat was associated with increased hot flashes [11, 12]. In addition, a study using ovariectomized (OVX) mice by Wang et al. confirmed an increase in tail skin temperature, body weight, and abdominal fat [13]. Therefore, these studies suggest that alleviating hot flashes may be possible due to body fat reduction.

Hormone replacement therapy (HRT) was preferred among various treatments because of its quick and immediate effect; however, after the Women's Health Initiative (WHI) announcement, the frequency of use decreased owing to various side effects and complications [14, 15]. Therefore, many researchers are exploring alternative medicines and methods that can replace HRT [16]. In Korea, the prescription danggui-yukhwang-tang (DYT) was widely used for fever, diabetes, perimenopausal syndrome, psoriasis, tuberculosis, and hyperthyroidism [18, 19]. In Chinese, DYT is called Dāngguī liù huángtāng (当归六**黄**汤). DYT consists of seven medicinal herbs: *Rehmanniae Radix Preparat* (RRP), *Astragali Radix* (AR), *Angelicae Gigantis Radix* (AGR), *Scutellariae Radix* (SR), *Rehmanniae Radix* (RR), *Phellodendri Cortex* (PC), and *Coptidis Rhizoma* (CR). However, no studies have been conducted to determine whether DYT is effective for treating menopausal obesity. Therefore, in this study, we investigated adipocyte differentiation and related genes using the 3T3-L1 pre-adipocyte cell line. Furthermore, we investigated the efficacy of DYT in postmenopausal obesity and hot flashes in an ovariectomized (OVX) high-fat diet (HFD) animal model.

Materials and methods

DYT preparation

The seven herbal medicines that constitute DYT were purchased from Gwangmyeong-dang (Daejeon, Korea) and approved by the botany specialist Dr. Byeong-Sub Ko (Korean Institute of Oriental Medicine, KIOM). DYT (26.2 g) was extracted by heating a mixture of seven herbal medicines (*Rehmanniae Radix Preparat* (24%), *Astragali Radix* (21%), *Angelicae Gigantis Radix* (17.6%), *Scutellariae Radix* (15.3%), *Rehmanniae Radix* (8.8%), *Phellodendri Cortex* (7.3%), and *Coptidis Rhizoma* (6%)), in a tenfold volume of water at 70 °C for 3 h. The extract was filtered through 0.4 μm filter paper (Whatman International, Maidstone, UK), and the filtered extract was evaporated using a rotary vacuum evaporator (N-1200A; Eyela, Tokyo, Japan) and then freeze-dried (yield 29.31% w/w). DYT extract (KIOM-PH-130026) was stored at the Korea Institute of Oriental Medicine (KIOM, Daejeon, Korea).

Chromatographic conditions for HPLC

The HPLC analysis was conducted with a Shimadzu LC-20A Prominence Series system (Shimadzu Corporation, Kyoto, Japan) equipped with a quaternary pump (LC-20AD), vacuum degasser (DGU-20A3R), auto-sampler (SIL-20A), column oven (CTO-20A), and photodiode-array detector (SPD-M20A). The chromatographic data were interpreted using Lab-Solutions Multi-PDA software. Chromatographic separation was performed on an Atlantis C18 (4.6*250 nm, 5um, Phenomenex). The column oven was maintained at 30 °C, the detection was conducted at $\lambda = 254$ nm, and online UV absorption spectra were recorded in the range of 190 to 400 nm. The gradient solution system was used for HPLC analysis for

Table 1 Linearity and contents (ug/mg) of DYT compounds

Compound name	t_R (min)	Equation (linear model)[a]	r^2 [b]	Mean (μg/mg)
5-HMF (**1**)	10.977	y = 74.905x—22.201	0.9994	0.8602
Nodakenin (**2**)	25.597	y = 20.545x—30.404	0.9991	2.9058
Baicalin (**3**)	30.601	y = 39.986x—41.79	0.9993	5.7878
Berberine (**4**)	36.097	y = 41.842x—76.286	0.9990	1.1507
Baicalein (**5**)	38.09	y = 63.327x – 156.2	0.9997	ND
Formononetin (**6**)	40.03	y = 63.853x – 9.8768	0.9988	ND
Wogonin (**7**)	43.29	y = 82,563x – 65.128	0.999	ND
Decrusin (**8**)	51.215	y = 142.02x—0.1912	0.9993	0.0168

a y: peak area at 254 nm; x: standard concentration (mg/mL). *b* r^2: coefficient of determination with 8 indicated points on the calibration curves

standard compound detection, and the analysis conditions are shown in Table 1. Flow rate was 1.0 mL/min and the injection volume were 1 µL. The standard compounds were obtained from Sigma-Aldrich (St. Louis, MO, USA). The eight chemical compounds had purities of ≥ 95% (Fig. 1a). The stock solution was prepared at concentrations of 1 mg/mL in 100% MeOH. The working solutions were serially diluted with methanol to obtain final concentrations of 0.0001 mg/mL and they were stored at 4 °C prior to analysis.

Cell viability assay

After overnight incubation in a 96-well plate at 2×10^3 cells/well, the 3T3-L1 pre-adipocyte cells were exposed to DYT (1, 10, 100, 200, 300, 400, 500, and 600 µg/mL) in the medium for 24 h. Cell viability was determined using an EZ-CyTox cell viability assay kit (Daeil Lab Service, Seoul, Korea). The absorbance was measured at 450 nm after the cells were incubated with EZ-CyTox solution (10 µL/well) for 4 h using a microplate reader (SynergyTM HT; BioTek® Instruments, Inc., Winooski, VT, USA).

Mouse pre-adipocytes (3T3-L1) culture and adipocyte differentiation

3T3-L1 pre-adipocytes were purchased from the American Type Culture Collection (ATCC, Rockville, MD, USA). Cells were maintained in DMEM containing 10% newborn calf serum (NBCS) and 0.5% antibiotics (penicillin 100 U/mL and streptomycin 100 µg/mL) medium (Gibco, Thermo Fisher Scientific, Waltham, MA, USA) in a humidified atmosphere of 5% CO_2 at 37 °C. For adipocyte differentiation, 3T3-L1 cells were incubated for two

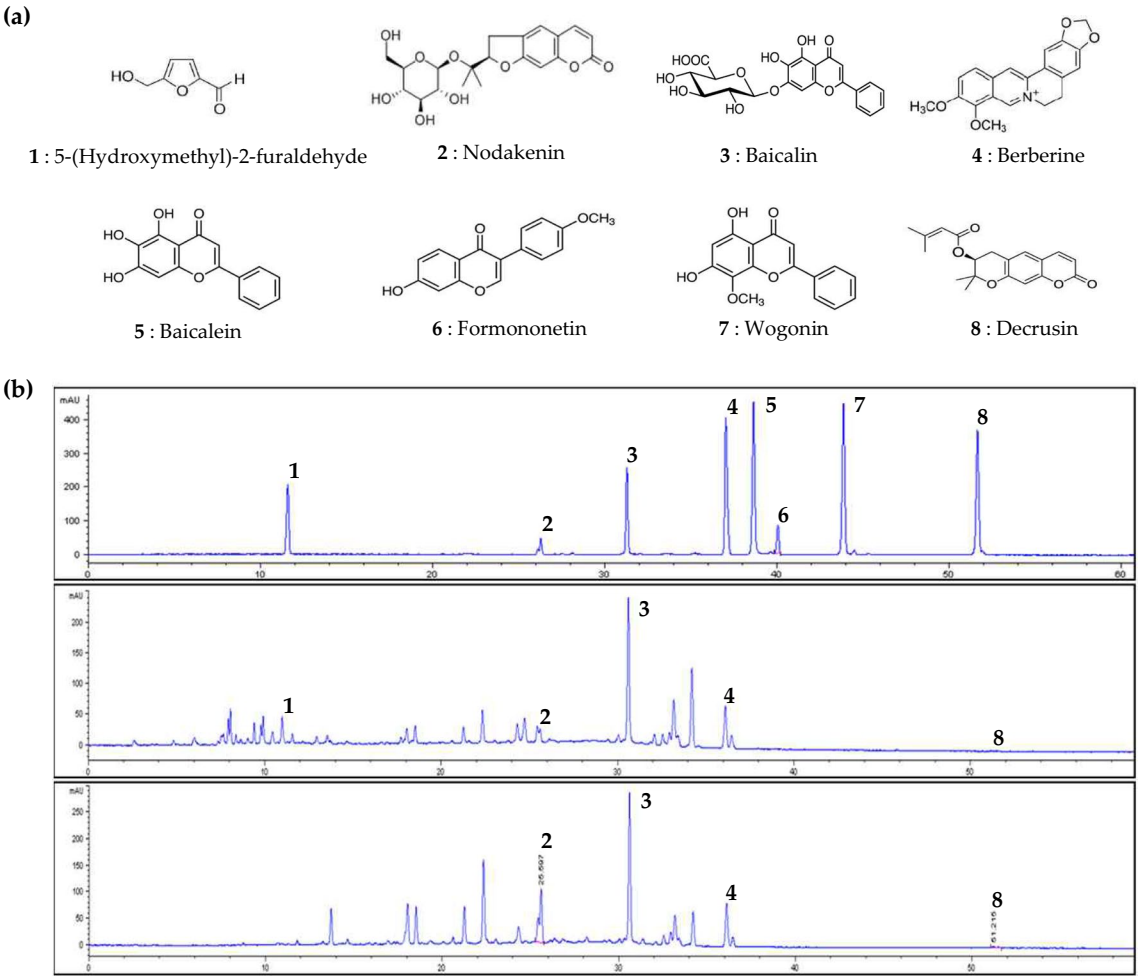

Fig. 1 The structures of eight compounds and HPLC analysis data of DYT extract. The HPLC chromatograms of the standard mixture 0.2 mg/mL, λ = 254 nm (**b**, top panel). The extracted DYT sample 1.0 mg/mL, λ = 254 nm (**b**, middle panel). The double check of nodakenin (2) and decrusin (8) from ARG was confirmed at 330 nm (**b**, lower panel)

days with 0.5 mM 3-isobutyl-1-ethylxanthine (IBMX), 1 μM dexamethasone, 1.67 μg/mL insulin (Sigma Aldrich, St Louis, MO, USA) in phenol-free DMEM/F12 (1:1) medium containing 10% charcoal-stripped FBS (CH-FBS, Gibco). It was then incubated with 1.67 μg/mL insulin for two days and then incubated in phenol-free DMEM containing 10% CH-FBS for four more days to observe lipid accumulation.

Oil red O staining and total lipid droplets quantification

To measure total intracellular lipid content, 3T3-L1 cells were stained by the Oil Red O (ORO) method as previously described [20]. Briefly, after cell differentiation, cells were washed twice with phosphate-buffered saline (PBS) and fixed with 10% formalin for 30 min at room temperature. Cells were washed with 60% isopropanol and stained with Oil Red O solution (Sigma-Aldrich, St Louis, MO, USA) for 1 h. After staining, the cells were sequentially washed with 70% ethanol and PBS and visualized under an optical microscope (Olympus, Tokyo, Japan). The stained lipid droplets were dissolved in 100% isopropanol and quantified using a microplate reader (BioTek Instruments, Inc.) by measuring the optical absorbance at 500 nm.

Quantitative real-time polymerase chain reaction (qReal-time PCR)

Total RNA was extracted from 3T3-L1 cells using the RNeasy Mini kit (QIAGEN Inc., Germantown, MD, USA), and the RNA concentration was assessed using a NanoDrop 2000 spectrophotometer (Thermo Scientific, Waltham, MA, USA). The extracted RNA was reverse-transcribed into cDNA using an iScript™ cDNA synthesis kit (Bio-Rad, Hercules, CA, USA). The mRNA expression levels were quantified by quantitative real-time PCR using SYBER Green PCR Master Mix and a 7500 Real-Time PCR system (Applied Biosystems, Foster City, CA, USA) according to the manufacturer's protocol. The primers targeting adipogenic markers were as follows: mouse C/EBPα sense, 5′-CGA CTT CTA CGA GGT GGA GC-3′; mouse C/EBPα anti-sense, 5′-TCG ATG TAG GCG CTG ATG TC-3′; mouse PPARγ sense, 5′-GGA AGC CCT TTG GTG ACT TTA TGG-3′; mouse PPARγ anti-sense, 5′-GCA GCA GGT TGT CTT GGA TGT C-3′; mouse FABP4 sense, 5′-AAT CAC CGC AGA CGA CAG-3′; mouse FABP4 anti-sense, 5′-ACG CCT TTC ATA ACA CAT TCC-3′; mouse GAPDH sense, 5′-TTG ATG CGA ACA ATC TCC AC-3′; mouse GAPDH anti-sense, 5′-CGT CCC GTA GAC AAA ATG GT-3′. Fold-changes are presented as $2-\Delta\Delta Ct$ ($\Delta\Delta Ct = \Delta Ct$ control $- \Delta$ Ct treatment).

Experimental animals and treatments

Female SD rats (5 weeks old) were purchased from Dooyeol Biotech Inc. (Seoul, Korea) and allowed to adapt to laboratory conditions (temperature, 20 ± 2 °C; relative humidity, 45 ± 5%; light/dark cycle, 12 h) for one week. After acclimatization at the experimental animal center of the Korea Institute of Oriental Medicine, anesthesia was induced using Avertin, and the skin was moved to the left and right to remove the ovary (OVX). A post-menopausal model was established by inducing symptoms for eight weeks after surgery. The rats (n = 56) were divided into eight groups (n = 7 sham, n = 7 OVX, n = 7 OVX + HFD, n = 7 OVX + HFD + E_2, n = 7 OVX + HFD + SV, n = 7 OVX + HFD + DYT500, n = 7 OVX + HFD + DYT1000, and n = 7 OVX + HFD + DYT1500). After two weeks of OVX, to assess the effects of DYT in preventing post-menopausal symptoms, rats were fed the AIN-76A diet as normal control (Sham), AIN-76A with 17β-estradiol (40 μg/kg/BW; Sigma-Aldrich, MO, USA) as a positive control I (OVX + HFD + E_2), AIN-76A with simvastatin (20 mg/kg BW; Sigma-Aldrich, MO, USA), and AIN-76A supplemented with DYT (DYT500; 500 mg/kg/BW, DYT1000; 1000 mg/kg/BW or DYT1500; 1500 mg/kg/BW) for 6 weeks. All animal experimental procedures were approved by the Ethics Committee of the Korea Institute of Oriental Medicine (Approved No. 17–029; Daejon, South Korea).

Cholesterol and triglyceride measurements in vitro and in vivo

The total triglyceride (TG) and total cholesterol (TC) contents of 3T3-L1 cells were measured using TG and TC quantification kits (ASAN Pharm, Co., Ltd, Seoul, Korea) [20]. Briefly, the treated cells were collected and vortexed by adding chloroform: isopropanol: tween-20 (7:11:0.1), and the extract was separated by centrifugation at 15,000×g for 10 min. The supernatant was transferred to a new tube and dried at 50 °C to completely remove the residual chloroform. After sufficiently dissolving the dried lipids in 150 μL of assay buffer, the TG and TC levels were measured using a microplate reader (BioTek® Instruments, Inc.) at 510 and 500 nm. The results were normalized to quantitative protein values.

Blood samples were collected directly from the inferior vena cava using a 1 mL syringe at the end of the experiment. Serum was obtained by centrifugation at 4000×g for 10 min and stored at −70 ℃ until use. Cholesterol (LDL-C, HDL-C, and TC) and TG concentrations were measured using an ELISA kit (BioVision Inc., Waltham, MA, USA), following the manufacturer's protocol. Briefly, 50 μL of serum collected from experimental animal groups or standard and 100 μL of biotinylated antibody cocktail was added to each well and allowed to react

for 2 h with 37 ℃. Subsequently, the wells were treated with 100 µL of HRP conjugate for 1 h, then reacted with 90 uL substrate for 15 min. Finally, 50 uL stop solution was treated and reacted, and then optic density was measured with a microplate reader at 450 nm within 10 min. A standard curve of each cholesterol was prepared and linear regression analysis was performed using PRISM software (GraphPad Inc., CA, USA) based on this standard curve.

Histological examinations of the liver and adipose tissue in ovariectomized high-fat diet animal model

Adipose tissues (peritoneal fat) were fixed with 10% neutral buffered formalin. These tissues were embedded in paraffin, sliced into 5 µm-thick sections, and stained with H&E (Sigma Aldrich, St Louis, MO, USA). For the Oil Red O staining of the liver tissue, OCT-embedded frozen tissues were sectioned at 10 µm, stained with 0.5% Oil Red O, and counterstained with hematoxylin. The cells were fixed in 4% paraformaldehyde solution for 10 min, rinsed with PBS, and stained with Oil Red O for 30 min. All tissue samples were evaluated and photographed under a light microscope in a blinded manner (BX43; Olympus). Images were captured using an Olympus DP-73 microscope (Olympus) and CellSens standard software (Olympus). Adipose and liver tissue images were analyzed using ImageJ software (ver. 1.51j8).

Tail temperature and infrared body temperature

The tail temperature of the rats was measured by attaching an infrared thermometer (Bioseb, Cheville, France; BIO-IRB153) to the tail. The surface temperature of the rat and its immediate surroundings were recorded using an infrared digital thermographic camera (IRIS-XP; Medicore, Gyunnggi-do, South Korea) placed 100 cm above the rats. The rats were photographed in the same gesture as possible in the recorded video.

Statistical analysis

Data are represented as the mean ± SD. Differences between means were obtained by conducting one-way ANOVA followed by Tukey's multiple comparison test using GraphPad Software (GraphPad Inc., CA, USA). $p < 0.05$ was considered statistically significant.

Results

Optimization of chromatographic conditions

To investigate the content of DYT compounds, 8 active compounds, each indicator component contained in a combination of herbal medicines, were quantitatively analyzed using HPLC/DAD. The active compounds to be analyzed were set based on Korean Pharmaceutical Affairs. The wavelength for detection was determined by comparing and analyzing the maximum UV absorbance profiles of each compound, and 254 nm was selected as the optimal single wavelength at which all eight compounds could be detected. The double check of each compounds was confirmed at 254 nm, 330 nm. The linear regression analysis of each compound with a corresponding standard was carried out, the results showed good linearity with r^2 values exceeding until 0.9990 to 0.9999, respectively. As a result, the three standard compounds selected, baicalein (**5**) and Formononetin (**6**), Wogonin (**7**) were not detected in DYT. Under these HPLC conditions, all compounds were free of interference from any other components and showed retention times of 10.97 (**1**), 25.75 (**2**), 30.60 (**3**), 36.09 (**4**), 38.09 (**5**), 40.03 (**6**), 43.29 (**7**), and 51.21 (**8**) min, respectively. The contents of the five compounds were successfully determined to be 0.8602 µg/mg for 1, 2.9058 µg/mg for 2, 5.7878 µg/mg for 3, 1.1507 µg/mg for 4, 0.0168 µg/mg for 8 (Fig. 1 and Table 1).

Effect of DYT on 3T3-L1 cell cytotoxicity

To investigate the cytotoxicity of DYT, 3T3-L1 cells were treated with various DYT concentrations (1, 10, 25, 50, 75, 100, 200, 300, 400, 500, and 600 µg/mL) for 24 h. As shown in Fig. 2a, cytotoxicity by DYT was not observed at any treatment concentration or time compared with the control group (untreated group). In contrast, significant cell proliferation was observed in the DYT 500 ($p < 0.01$) and 600 µg/mL ($p < 0.001$) treatment groups for 24 h. Cytotoxicity was not observed at 600 µg/mL DYT, but it did not completely dissolve in water; hence, the final treatment concentration was determined to be 500 µg/mL.

Inhibitory effect of DYT on lipid production and accumulation in 3T3-L1 cells

Based on our cell cytotoxicity results, we examined the anti-adipogenic effect of DYT in vitro using 3T3-L1 preadipocyte cells (Fig. 2b). First, we induced 3T3-L1 cell differentiation by treating the cells with E_2 and DYT at the indicated concentrations in differentiation medium supplemented with charcoal-stripped FBS (CH-FBS). Oil Red O (ORO) staining of lipid droplets in differentiated adipocytes revealed significant inhibition of lipid droplet accumulation in the E_2 treated group compared to that in the control group ($p < 0.05$). Similarly, a significant dose-dependent inhibition of lipid droplet accumulation was observed in the DYT treatment group ($p < 0.001$), and the DYT 400 and 500 µg/mL treatment groups exhibited a higher lipid droplet accumulation inhibitory effect than the E_2 group ($p < 0.001$) (Fig. 2c, d). In addition, total triglyceride (TG) and total cholesterol (TC) levels were significantly reduced by E_2 treatment compared with those

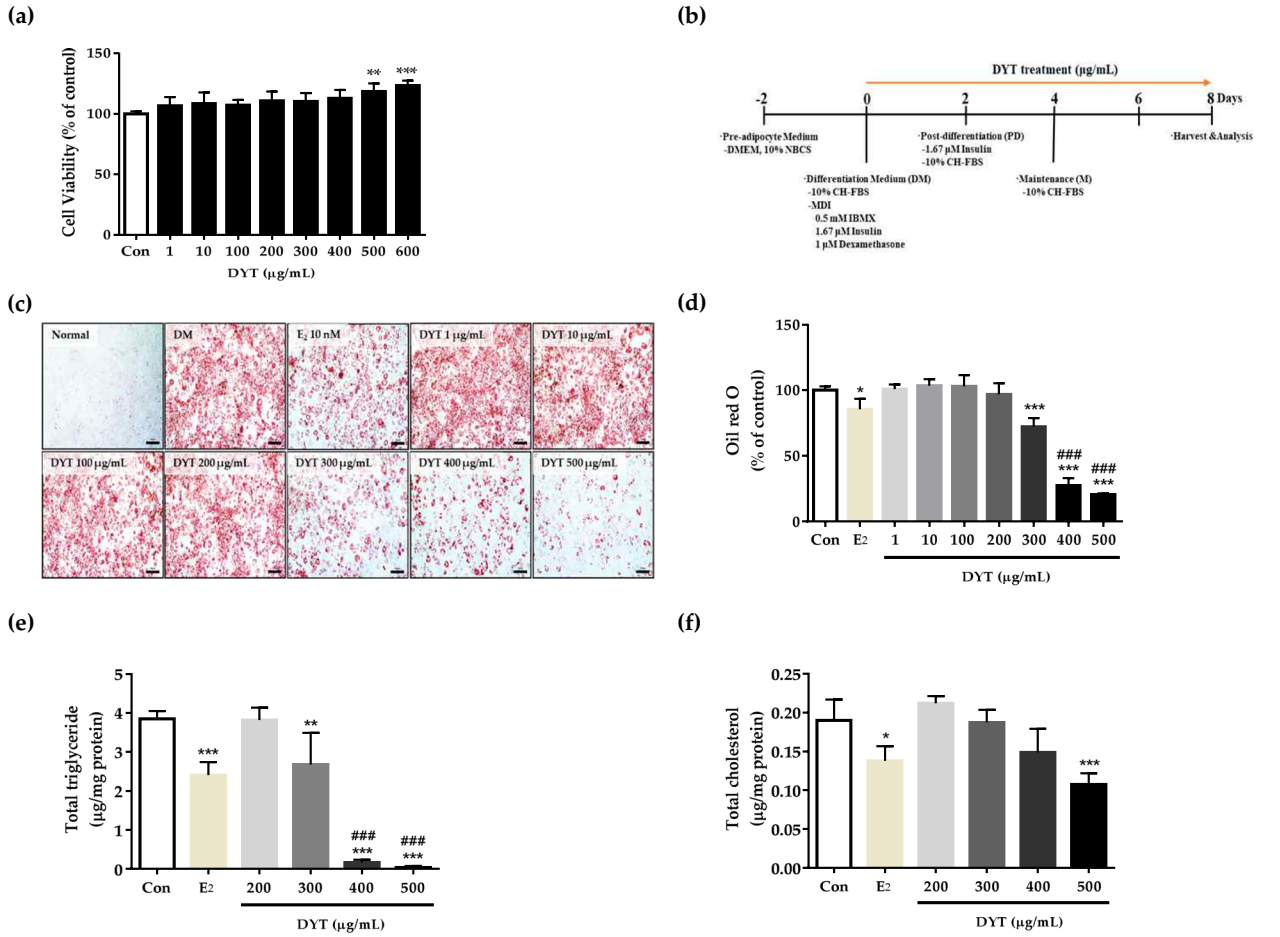

Fig. 2 Effect of DYT on cell viability and anti-adipogenesis in 3T3-L1 cells. Cell viability by DYT in 3T3-L1 cells (**a**). Data are presented as mean ± SD of four experiments. ** $p < 0.01$, *** $p < 0.001$ *vs.* control. A brief overview of 3T3-L1 differentiation (**b**). Optical microscope images of intracellular lipid droplets of differentiated 3T3-L1 cells (× 200) (**c**). Graph representing the quantification of lipid accumulation in each treatment group (**d**). Data are presented as mean ± SD of four experiments. * $p < 0.05$, *** $p < 0.001$ *vs.* control, ### $p < 0.001$ *vs.* E_2. The quantification of total triglyceride (TG) for each treatment group (**e**). The quantification of total cholesterol (TC) for each treatment group (**f**). The results are presented as the mean ± SD of four independent experiments. * $p < 0.05$, ** $p < 0.01$, *** $p < 0.001$ *vs.* control., ### $p < 0.001$ *vs.* E_2

in the control group ($p < 0.001$ and $p < 0.05$, respectively). In the DYT treatment group, the TG level showed a significant decrease in a DYT dose-dependent manner, and similar to the ORO result, a better decrease was observed at DYT 400 and 500 μg/mL than E_2 ($p < 0.001$). Finally, a significant decrease in TC levels was observed at DYT 500 μg/mL compared with that in the control group ($p < 0.001$) (Fig. 2e, f). These results suggest that DYT has an inhibitory effect on adipocyte differentiation or lipid accumulation in estrogen deficiency and has an effect equal to or greater than that of E_2 in terms of inhibitory efficacy.

Inhibitory effect of DYT on the expression of adipogenesis regulatory genes

Adipocyte-specific transcription factors and regulatory genes are closely related to adipocyte differentiation. To investigate the effects of DYT on the differentiation-related genes of 3T3-L1 pre-adipocytes, the expression levels of *PPARγ*, *C/EBPα*, and *FABP4* mRNA were analyzed by quantitative real-time PCR (qRT-PCR). As shown in Fig. 3, *PPARγ*, *C/EBPα*, and *FABP4* mRNA levels were significantly lower in the E_2 treatment group than in the control group ($p < 0.05$). In the DYT treatment group, the expression of C/EBP*α* was dramatically reduced at 300 μg/mL concentrations or higher (Fig. 3b), whereas the expression of PPARγ and FABP4 was significantly reduced at 400 μg/mL concentrations or higher (Fig. 3a, c). Furthermore, compared with the E_2 treatment

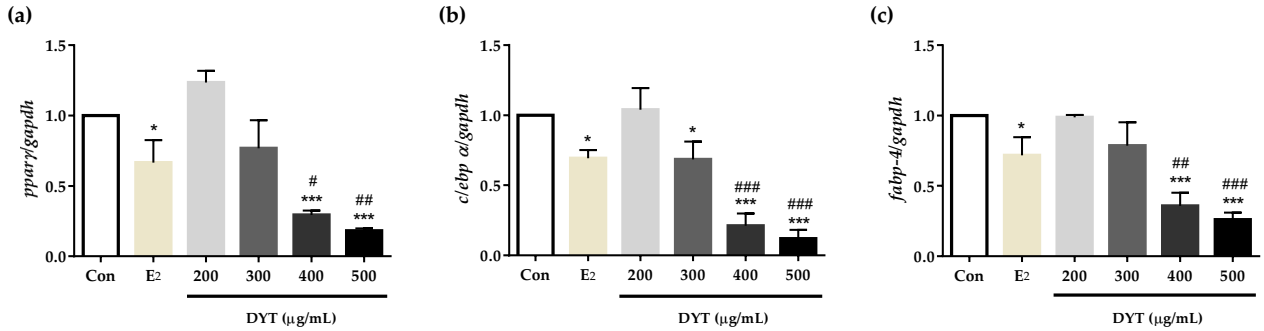

Fig. 3 Effect of DYT on the expression of adipogenic-related mRNA in differentiated 3T3-L1 cells. The relative expression levels of PPARγ (**a**), C/EBP*α* (**b**), and FABP4 (**c**) mRNA by qRT-PCR analysis. The data were normalized using the GAPDH as internal control. The results are presented as the mean ± SD of three independent experiments. * $p < 0.05$, *** $p < 0.001$ *vs.* control., # $p < 0.05$, ## $p < 0.01$, ### $p < 0.001$ *vs.* E_2

group, PPARγ, C/EBPα, and FABP4 mRNA levels were significantly decreased at 400 and 500 μg/mL. These results suggest that DYT has the potential to improve lipid production and accumulation due to E_2 reduction and is a mechanism for the inhibition of key factors such as PPARγ, C/EBPα, and FABP4, which are factors that regulate adipocyte differentiation.

Weight(s) and serum lipid profile in an animal model

To determine whether DYT (500, 1000, or 1500 mg/kg BW) treatment could improve post-menopausal symptoms in ovariectomy (OVX), the rats were treated with E_2, simvastatin (SV), or DYT (Fig. 4a). In the ovariectomized and high-fat diet model experimental groups, the body weights were significantly elevated compared to the sham group. Weight gain was significantly decreased in the DYT-treated group compared to the OVX + HFD group (Fig. 4b). Uterine weight was significantly decreased in all OVX groups (Fig. 4c). The weight of intraperitoneal fat was significantly higher in the OVX and OVX + HFD groups than in the sham group and lower than that of the OVX + HFD group in the group treated with E_2 and DYT1500 (Fig. 4d). Daily food intake was significantly increased in the OVX group compared to the sham group and decreased significantly in the E_2 and DYT treatment groups compared to the OVX group. For the HFD-fed group, there was a tendency to increase; however, the difference was not statistically significant (Fig. 4e). The serum levels (s) of TG were also elevated in the OVX and OVX + HFD groups, and the levels were significantly reduced in the DYT-treated group (500, 1000, and 1500 mg/kg BW) (Fig. 5a). In the serum cholesterol profile, TC was significantly increased in the OVX or OVX + HFD group compared to the sham group and was significantly reduced in the DYT 1000 and 1500 mg/kg/BW treatment groups (Fig. 5b). In addition, LDL-cholesterol levels were high in the OVX and OVX + HFD groups, and the lowest level was observed in the treatment groups treated with 500, 1000, and 1500 mg/kg DYT (Fig. 5c). For HDL-cholesterol, a significant decrease was observed only in the OVX + HFD group compared to the sham group, whereas a significant increase was observed in the SV and DYT 1500 mg/kg BW treatment groups (Fig. 5d).

Inhibitory effect of DYT on fat accumulation in liver and adipose tissue

We further investigated whether DYT inhibits fat accumulation in the liver and peritoneal fat tissue. First, as a result of staining with ORO to confirm fat accumulation in the liver tissue, an increase in fat accumulation was observed in the OVX and OVX + HFD groups compared to the sham group. In particular, an increase in fat accumulation was observed in the OVX + HFD group compared to that in the OVX group. This fat accumulation improved in the E_2 and SV treatment groups, and a dose-dependent decrease in fat accumulation was observed in the DYT treatment group (Fig. 6a). Histological analysis of peritoneal adipose tissue showed that the size of adipose tissue was significantly increased in the OVX + HFD treatment group, and the number of adipose tissues was significantly decreased. Similar to the liver tissue results, significant improvement was confirmed in the E_2 and SV treatment groups, and a significant dose-dependent improvement effect of DYT treatment was also observed (Fig. 6b).

The tail- or infrared body-temperature

To investigate the anti-hot flash effects of DYT on body temperature, we measured the body (tail) or whole-body infrared temperature six weeks after DYT treatment in OVX + HFD rats. The tail temperature was elevated in the OVX + HFD group, and its induction was decreased by E_2 or DYT treatment in OVX + HFD rats. The tail temperature also fluctuated in the OVX group. However, this difference was not significant. In addition, changes in

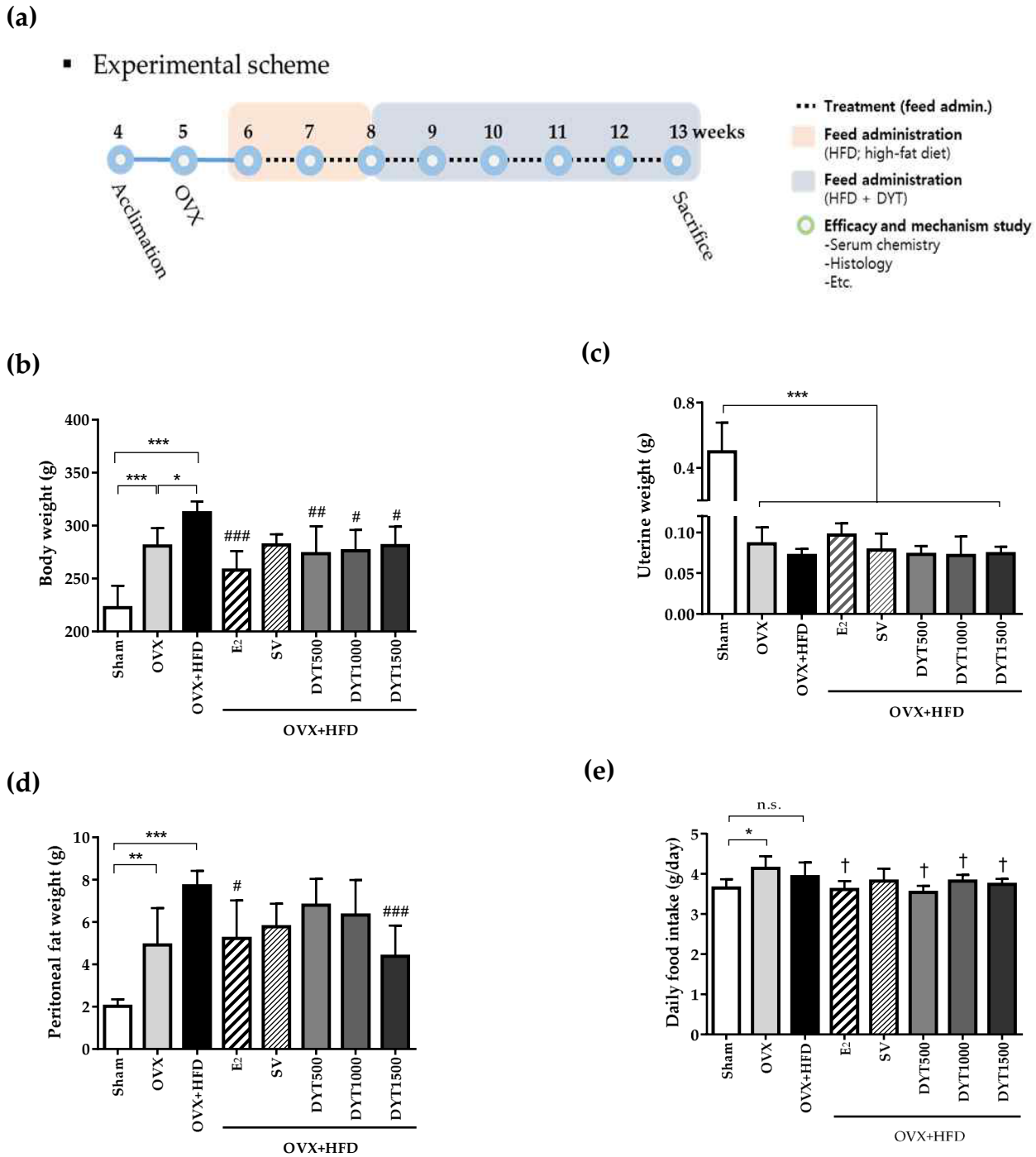

Fig. 4 Effect of DYT in OVX or OVX + HFD rat models. A brief overview of the animal model experiments (**a**). Body weight (**b**), uterine weight (**c**), peritoneal fat weight (**d**), and daily food intake (**e**). Normal diet group: Sham; ovariectomized normal diet group: OVX; ovariectomized high-fat diet: OVX + HFD; ovariectomized high-fat diet plus 17β-estradiol 40 μg/kg: OVX + HFD + E_2; ovariectomized high-fat diet plus simvastatin 20 mg/kg: OVX + HFD + SV; ovariectomized high-fat diet plus 500 mg/kg DYT: OVX + HFD + DYT500; ovariectomized high-fat diet plus 1000 mg/kg DYT: OVX + HFD + DYT1000; ovariectomized high-fat diet plus 1500 mg/kg DYT: OVX + HFD + DYT1500. Data are presented as mean ± SD (n = 7). * $p < 0.05$, ** $p < 0.01$, *** $p < 0.001$ *vs.* sham or OVX group., † $p < 0.05$ vs. OVX group., # $p < 0.05$, ## $p < 0.01$, ### $p < 0.001$ *vs.* OVX + HFD group

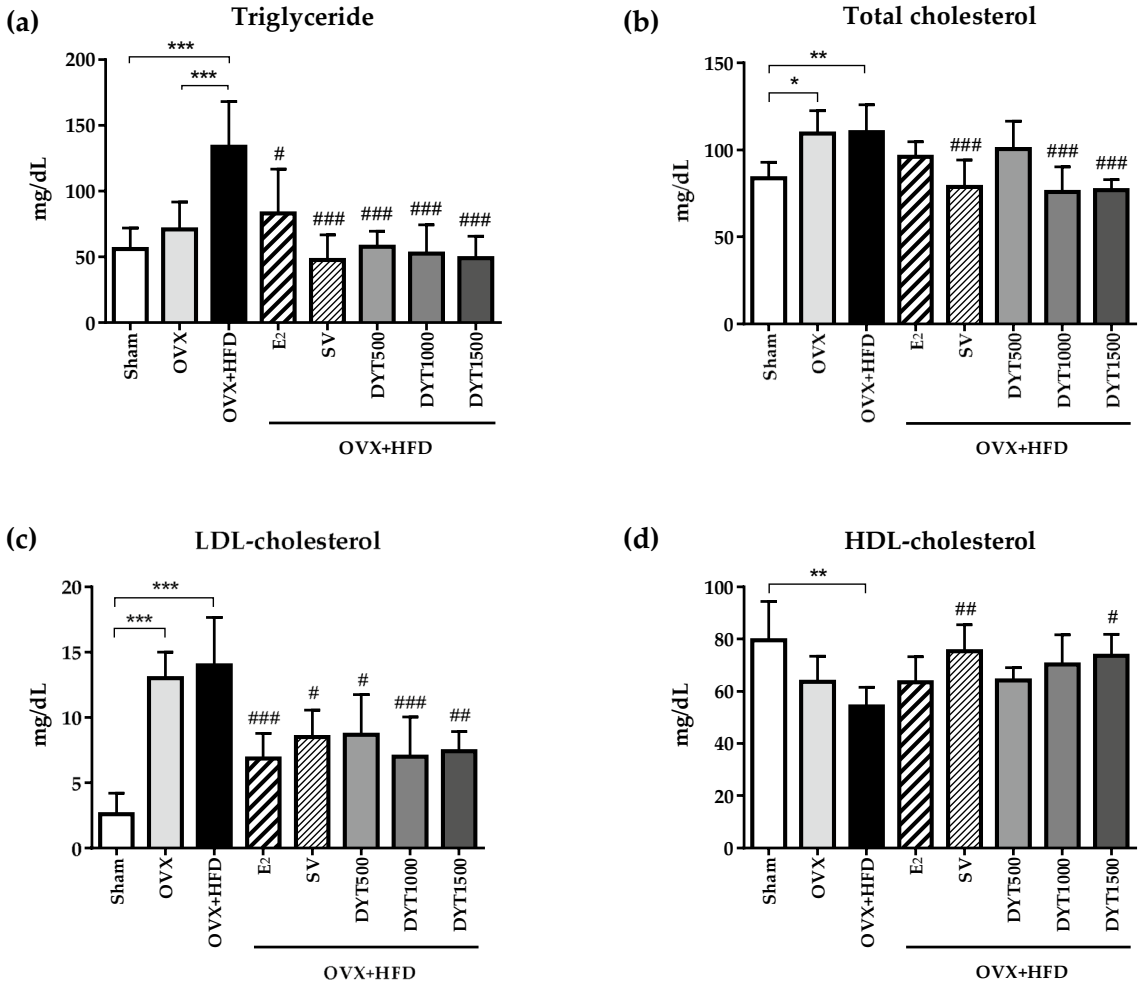

Fig. 5 Effect of DYT on the serum lipid profile in ovariectomized high-fat diet animal model. Triglyceride (**a**), total cholesterol (**b**), LDL-cholesterol (**c**), and HDL-cholesterol (**d**) were measured using a competitive enzyme-linked immunosorbent assay, and data was analyzed using software PRISM (Graphpad; CA, USA). Data are presented as mean ± SD (n = 7). * $p < 0.05$, ** $p < 0.01$, *** $p < 0.001$ *vs.* sham or OVX group., # $p < 0.05$, ## $p < 0.01$, ### $p < 0.001$ vs. OVX + HFD group

temperature using infrared thermometers were observed in different patterns in the torso and tail, which were observed only in the OVX + HFD group (Fig. 7). The tail temperatures were elevated in the OVX or OVX + HFD groups, and its induction was effectively reduced by E_2 or DYT treatment. However, torso temperature tended to be decreased in the OVX + HFD group and slightly increased by DYT treatment (Fig. 7a, b).

Discussion

This study aimed to evaluate whether DYT could improve menopausal obesity. In vitro results using 3T3-L1 cells showed that DYT improved adipocyte differentiation, lipid accumulation, and TG and TC levels through downregulation of *PPARγ*, *C/EBPα*, and *FABP4* mRNA. We also confirmed the DYT-induced improvement in body mass, serum parameters, histological lesions, and clinical symptoms of menopausal obesity in HFD-fed animal models after OVX. In addition, an improvement in tail skin temperature with weight gain was confirmed. These findings imply that DYT has therapeutic potential in the prevention of obesity by reducing the weight increase caused by estradiol deficiency.

Previous studies have suggested that estrogen deficiency can lead to obesity. Due to the local differences in adipocytes for each sex hormone receptor, estrogen induces mainly peripheral fat storage via the receptors ER*α*, whereas androgens contribute to visceral abdominal fat accumulation [21, 22]. The decrease in estrogen following menopause causes a relative androgen excess, leading to a redistribution of body fat

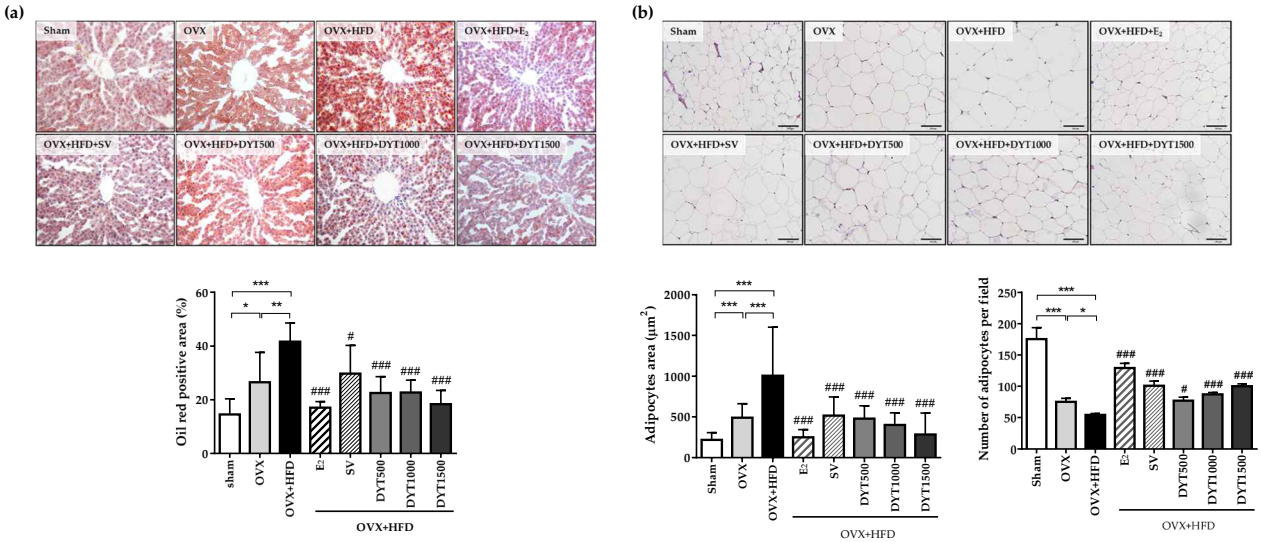

Fig. 6 Effect of DYT on fat accumulation in liver and adipose tissue. The accumulation of lipid droplets in the liver tissue was evaluated by ORO staining (× 400), and ORO-positive areas were analyzed using ImageJ software (**a**). The size and number of adipocytes in the adipose tissue were evaluated by H&E staining (× 400), and the size and number of adipocytes were analyzed using ImageJ software (**b**). Data are presented as the mean ± SD (n = 7). *$p < 0.05$, **$p < 0.01$, ***$p < 0.001$ vs. sham or OVX group, #$p < 0.05$, ###$p < 0.001$ vs. OVX + HFD group

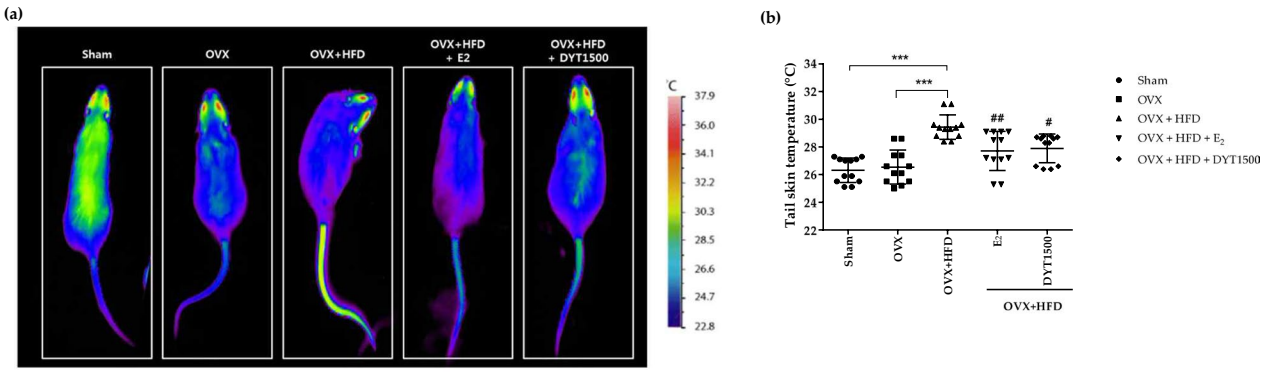

Fig. 7 Effect of DYT on the tail- or body- temperature. Tail skin and infrared body temperatures were evaluated with an infrared thermometer or thermography, respectively (**a**), and data of tail-skin temperature was analyzed using software PRISM (Graphpad; CA, USA) (**b**). Data are presented as mean ± SD (n = 7). ***$p < 0.001$ vs. Sham group or OVX group. #$p < 0.05$, ##$p < 0.01$ vs. OVX + HFD group

(mainly visceral abdominal fat) [22–24]. In addition, an increase in all-trans-retinol 13,14-reductase (RET-SAT), which promotes adipogenesis in adipocytes, and adipose tissue lipoprotein lipase (AT-LPL), which is involved in FFA production, absorption, and storage, were reported in a study in OVX mice [25–28]. Owing to these effects, the increased FFA produced from the excessively accumulated visceral abdominal fat flows into the liver and increases insulin resistance [29]. Furthermore, decreased estrogen synthesis due to ovarian dysfunction increases CVD prevalence by increasing LDL-C, a substrate for E_2, and decreasing HDL-C [27]. In this study, body weight, daily food intake, peritoneal fat weight, TG, TC, LDL-C, and HDL-C levels were improved by DYT in ovariectomized HFD-fed animal model. In particular, weight gain increased in the OVX + HFD group compared to that in the OVX group, but there was no significant change in the daily food intake, confirming that estrogen decrease due to ovariectomy was the main cause (Fig. 4b and e). In addition, uterine weight decreased in the ovarian removal group. This suggests that DYT does not induce endocrine disturbances (Fig. 4c). In addition, histological analysis of adipose tissue confirmed that

DYT decreased the area of peritoneal adipocytes and increased the number of adipocytes. Similarly, inhibition of lipid accumulation in the liver tissue by DYT was confirmed.

PPARγ plays a key role in adipocyte differentiation and maturation [30]. Activated C/EBPα by C/EBPβ and C/EBPδ, which are expressed at the early stage of adipocyte differentiation, induce mutual expression with PPARγ and cooperate with the activation of adipocyte genes such as FAS and FABP4 [7]. In premenopausal women, PPARγ activity is downregulated by estrogen-activated ERα, and estrogen loss with menopause increases the effect of PPARγ to promote weight gain [31]. Therefore, we induced 3T3-L1 differentiation by treating DYT in a phenol-free medium containing CH-FBS to block hormonal interference (Fig. 2b). It was confirmed that adipocyte differentiation and lipid accumulation were suppressed (Fig. 2c and d), and the expression of important differentiation regulators such as PPARγ, C/EBPα, and FABP4 was suppressed (Fig. 2e and f). Therefore, the anti-obesity efficacy of DYT suggests that the inhibition of adipocyte differentiation by downregulation of FABP4 due to decreased activity of PPARγ and C/EBPα is an important mechanism.

Thurston et al. reported that hot flashes were correlated with fat accumulation, such as abdominal and visceral fat, and that obesity suppression could be helpful in the treatment of hot flashes due to menopause [11]. Additionally, it has been reported that tail skin temperature may be representative of hot flashes in ovariectomized (OVX) mice. Therefore, in our study, it was possible to confirm the increase in the tail skin temperature of the group fed HFD to OVX rather than OVX, and it was confirmed that E_2 and DYT lowered the temperature increase. These results suggest that menopausal obesity may cause an increase in hot flashes, which may be alleviated by DYT through obesity suppression. Taken together, our results using the OVX-HFD animal model demonstrate that DYT can help improve lipid metabolism and alleviate menopausal symptoms such as hot flashes by inhibiting key factors related to lipid accumulation in menopausal obesity. Therefore, we report for the first time that DYT can be used as a potentially good treatment option for menopausal obesity and its resulting metabolic syndrome.

Acknowledgements
This work was supported by the Korea Institute of Oriental Medicine (Grant Nos. KSN 1515290 and KSN20224314)

Author contributions
Conceptualization, investigation, writing-original draft preparation, and writing-review and editing, DHJ and HY; investigation and data analysis JTH; conceptualization, supervision, project administration, writing, review, and editing, B-SK. All author read and approved the final manuscript.

Funding
This research was funded by the Korea Institute of Oriental Medicine (Grant Nos. KSN 1515290 and KSN20224314).

Availability of data and materials
The datasets used and/or analyzed during the current study available from the corresponding author on reasonable request.

Declarations

Competing interests
The authors declare that they have no competing interests.

Received: 26 September 2022 Accepted: 19 December 2022
Published online: 27 January 2023

References

1. Gold EB (2011) The timing of the age at which natural menopause occurs. Obstet Gyn Clin N Am 38(3):425–440
2. Burger HG, Hale GE, Dennerstein L, Robertson DM (2008) Cycle and hormone changes during perimenopause: the key role of ovarian function. Menopause 15(4 Pt 1):603–612
3. Takahashi TA, Johnson KM (2015) Menopause. Med Clin N Am 99(3):521–534
4. Fait T (2019) Menopause hormone therapy: latest developments and clinical practice. Drugs Context 8:212551
5. Ko SH, Jung Y (2021) Energy metabolism changes and dysregulated lipid metabolism in postmenopausal women. Nutrients 13(12):4556
6. Ebong IA, Wilson MD, Appiah D, Michos ED, Racette SB, Villablanca A, Breathett K, Lutsey PL, Wellons M, Watson KE, Chang P, Bertoni AG (2022) Relationship between age at menopause, obesity, and incident heart failure: the atherosclerosis risk in communities study. J Am Heart Assoc 11(8):e024461
7. Moseti D, Regassa A, Kim WK (2016) Molecular regulation of adipogenesis and potential anti-adipogenic bioactive molecules. Int J Mol Sci 17(1):124
8. Weigt C, Hertrampf T, Kluxen FM, Flenker U, Hülsemann F, Fritzemeier KH, Diel P (2013) Molecular effects of ER alpha- and beta-selective agonists on regulation of energy homeostasis in obese female Wistar rats. Mol Cell Endocrinol 377(1–2):147–158
9. Chu R, van Hasselt A, Vlantis AC, Ng EK, Liu SY, Fan MD, Ng SK, Chan AB, Liu Z, Li XY, Chen GG (2014) The cross-talk between estrogen receptor and peroxisome proliferator-activated receptor gamma in thyroid cancer. Cancer 120(1):142–153
10. Boldarine VT, Pedroso AP, Brandão-Teles C, LoTurco EG, Nascimento CMO, Oyama LM, Bueno AA, Martins-de-Souza D, Ribeiro EB (2020) Ovariectomy modifies lipid metabolism of retroperitoneal white fat in rats: a proteomic approach. Am J Physiol Endocrinol Metab 319(2):e427–e437
11. Thurston RC, Sowers MR, Sutton-Tyrrell K, Everson-Rose SA, Lewis TT, Edmundowicz D, Matthews KA (2008) Abdominal adiposity and hot flashes among midlife women. Menopause 15(3):429–434
12. Su HI, Sammel MD, Springer E, Freeman EW, DeMichele A, Mao JJ (2010) Weight gain is associated with increased risk of hot flashes in breast cancer survivors on aromatase inhibitors. Breast Cancer Res Treat 124(1):205–211
13. Wang W, Yang Q, Zhou C, Jiang H, Sun Y, Wang H, Luo X, Wang Z, Zhang J, Wang K, Jia J, Qin L (2022) Transcriptomic changes in the hypothalamus of ovariectomized mice: data from RNA-seq analysis. Ann Anat 241:151886
14. Webber L, Anderson RA, Davies M, Janse F, Vermeulen N (2017) (2017) HRT for women with premature ovarian insufficiency: a comprehensive review. Hum Reprod Open. 2:hox007
15. Cagnacci A, Venier M (2019) The controversial history of hormone replacement therapy. Medicina (Kaunas) 55(9):602
16. Posadzki P, Lee MS, Moon TW, Choi TY, Park TY, Ernst E (2013) Prevalence of complementary and alternative medicine (CAM) use by menopausal women: a systematic review of surveys. Maturitas 75(1):34–43

17. Cao H, Li S, Xie R, Xu N, Qian Y, Chen H, Hu Q, Quan Y, Yu Z, Liu J, Xiang M (2018) Exploring the mechanism of dangguiliuhuang decoction against hepatic fibrosis by network pharmacology and experimental validation. Front Pharmacol 9:187
18. Liu T, Cao H, Ji Y, Pei Y, Yu Z, Quan Y, Xiang M (2015) Interaction of dendritic cells and T lymphocytes for the therapeutic effect of Dangguiliuhuang decoction to autoimmune diabetes. Sci Rep 5:13982
19. Nguyen LTH, Ahn SH, Nguyen UT, Yang IJ (2018) Dang-Gui-Liu-Huang Tang a traditional herbal formula, ameliorates imiquimod-induced psoriasis-like skin inflammation in mice by inhibiting IL-22 production. Phytomedicine 47:48–57
20. Go H, Ryuk JA, Hwang JT, Ko BS (2017) Effects of three different formulae of Gamisoyosan on lipid accumulation induced by oleic acid in HepG2 cells. Integr Med Res 6(4):395–403
21. Frank AP, de Souza SR, Palmer BF, Clegg DJ (2019) Determinants of body fat distribution in humans may provide insight about obesity-related health risks. J Lipid Res 60(10):1710–1719
22. Perry A, Wang X, Goldberg R, Ross R, Jackson L (2013) Androgenic sex steroids contribute to metabolic risk beyond intra-abdominal fat in overweight/obese black and white women. Obesity (Silver Spring) 21(8):1618–1624
23. Razmjou S, Abdulnour J, Bastard JP, Fellahi S, Doucet É, Brochu M, Lavoie JM, Rabasa-Lhoret R (2018) Body composition, cardiometabolic risk factors, physical activity, and inflammatory markers in premenopausal women after a 10-year follow-up: a MONET study. Menopause 25(1):89–97
24. Ko SH, Kim HS (2020) Menopause-associated lipid metabolic disorders and foods beneficial for postmenopausal women. Nutrients 12(1):202
25. Moise AR, Kuksa V, Imanishi Y, Palczewski K (2004) Identification of all-trans-retinol: all-trans-13,14-dihydroretinol saturase. J Biol Chem 279(48):50230–50242
26. Weber P, Flores RE, Kiefer MF, Schupp M (2020) Retinol saturase: more than the name suggests. Trends Pharmacol Sci 41(6):418–427
27. Dmitruk A, Czeczelewski J, Czeczelewska E, Golach J, Parnicka U (2018) Body composition and fatty tissue distribution in women with various menstrual status. Rocz Panstw Zakl Hig 69(1):95–101
28. Yang A, Mottillo EP (2020) Adipocyte lipolysis: from molecular mechanisms of regulation to disease and therapeutics. Biochem J 477(5):985–1008
29. Mumusoglu S, Yildiz BO (2019) Metabolic syndrome during menopause. Curr Vasc Pharmacol 17(6):595–603
30. Lehrke M, Pascual G, Glass CK, Lazar MA (2005) Gaining weight: the Keystone Symposium on PPAR and LXR. Genes Dev 19(15):1737–1742
31. Lundholm L, Zang H, Hirschberg AL, Gustafsson JA, Arner P, Dahlman-Wright K (2008) Key lipogenic gene expression can be decreased by estrogen in human adipose tissue. Fertil Steril 90(1):44–48

Publisher's Note